# Measurements of Saturation Densities in Critical Region of Pentafluoroethyl Methyl Ether (245cbEβγ)[1]

Yasutaka Yoshii,[2,4] Masao Mizukawa,[2] Januarius V. Widiatmo,[2,3] and Koichi Watanabe[2]

[1] Paper presented at the Fourteenth Symposium on Thermophysical Properties, June 25-30, 2000, Boulder, Colorado, U.S.A.

[2] Department of System Design Engineering, Faculty of Science and Technology, Keio University, 3-14-1, Hiyoshi, Kohoku-ku, Yokohama 223-8522, Japan

[3] Permanent Researcher at Agency for the Assessment and Application of Technology, Jl. M. H. Thamrin No. 8, Jakarta 10340, Indonesia.

[4] To whom correspondence should be addressed.

**Abstract**

We have measured 10 saturated vapor and 13 liquid densities in the critical region of pentafluoroethyl methyl ether, $CF_3CF_2OCH_3$ (245cbEβγ), based on the direct visual observation of the meniscus disappearance in an optical cell. The critical temperature and density have been determined by taking into consideration the meniscus disappearing level of the sample within the optical cell as well as the intensity of the critical opalescence. The experimental uncertainties of saturation temperature and density measurements were estimated to be within ±12 mK and 0.5 - 4.0 $kg \cdot m^{-3}$, while those of the critical temperature and density values determined are to be within ±17 mK and 3 $kg \cdot m^{-3}$, respectively. We have also determined the critical exponent, $\beta$, and the critical amplitude, $B$, on the basis of the vapor-liquid coexistence curve correlation developed.

Key words: Critical amplitude; Critical exponent; Critical parameter; Pentafluoroethyl methyl ether; Vapor-liquid coexistence curve.

## Introduction

The Research Institute of Innovative Technology for the Earth (RITE), Kyoto, Japan has been challenging to synthesize several candidates for the long-term alternatives among the fluorinated ethers under the Development of New Refrigerant, Blowing Agent and Cleaning Solvent for Effective Use of Energy Project[1]. Those are expected with a possibility to be the new-generation alternative refrigerants, because of their zero ODP values and negligible GWP values. One of the most promising fluorinated ethers is pentafluoroethyl methyl ether, $CF_3CF_2OCH_3$ (245cbEβγ), to replace dichloro-tetrafluoroethane, $CClF_2$-$CClF_2$ (R-114), especially for high-temperature vapor-compression heat pump applications. However, the reliable experimental information about the thermodynamic properties of this substance is still very limited even for the critical parameters that are important in predicting various thermodynamic properties and in formulating equations of state.

This paper reports measurements of the saturation densities in the critical region, and the determined critical temperature and density values. In addition, we have also developed a vapor-liquid coexistence curve correlation from which the critical exponent, $\beta$, and the critical amplitude, $B$, have been determined.

## Experimental Section

We measured the saturation densities in the vicinity of the critical point by means of a direct observation of the meniscus (vapor-liquid coexistence interface) disappearance

and critical opalescence. A phenomena that sample refrigerant colored dark brown or black in the vicinity of the critical point is called the critical opalescence, since only the light with longer wavelength can penetrate the sample fluid which would be composed of molecular clusters near the critical point. In addition to the critical opalescence, we have also paid full attention to the meniscus disappearing level.

Special caution was paid to establish a uniform temperature field for a certain period of time in order to maintain well-established thermal equilibrium condition. When the average sample density in the optical cell is greater than the critical density, the sample meniscus locates just a little higher than the middle of the optical cell and critical opalescence becomes intense in the liquid phase. When it is smaller than the critical density, on the other hand, the meniscus locates just a little lower than the middle of the optical cell and critical opalescence becomes intense in the vapor phase. The temperature at which the sample meniscus disappears is regarded as saturation temperature corresponding to the average sample fluid density. By repeating these measurements along different isochores in the vicinity of the critical point, it becomes feasible to determine the critical temperature and critical density rather precisely with smaller uncertainties.

This experimental apparatus used for the present measurements has originally been reported by Okazaki *et al.*[2] and Tanikawa *et al.*[3] made some modifications. Since then, we have completed a series of similar measurements with respect to HCFC and HFC refrigerants and their mixtures including R-23 (Okazaki *et al.*[2]), R-502 (Higashi *et al.* [4]), R-12 + R-22 (Higashi *et al.*[5]), R-22 + R-114 (Higashi *et al.*[6]), R-152a (Higashi *et al.*[7]), Halon-1301 + R-114 (Higashi *et al.*[8]), R-134a (Kabata *et al.*[9]), R-123 (Tanikawa *et al.*[3]), R-142b (Tanikawa *et al.*[10]), R-134 (Tatoh *et al.*[11]), R-125 (Kuwabara *et al.*[12]), R-32

(Kuwabara *et al.*[12]), R-236ea (Aoyama *et al.*[13]), R-143a (Aoyama *et al.*[13]), R-134a (Aoyama *et al.*[13]), R-125 + R-134a (Kishizawa *et al.*[14]), and R-32 + R-143a (Kishizawa *et al.*[14]).

Figure 1 shows a schematic experimental apparatus. The apparatus consists of three vessels: an optical cylindrical cell (A) with two synthetic sapphire windows at both ends for observing the meniscus of sample refrigerant, an expansion vessel (B) for making expansion, and a supplying vessel (C) for supplying the sample refrigerant. The inner volumes of the optical cell, the expansion vessel, and the supplying vessel are 11.108±0.006 $cm^3$, 6.297±0.007 $cm^3$, and 77.457±0.009 $cm^3$, respectively. These three vessels are made of stainless steel and all are installed on a horizontal frame that can be rocked. This assembly is set in a thermostated fluid bath (I) where silicone oil is filled and circulated by a stirrer (L). Since the cylindrical optical cell (A) is considered being a constant-volume cell in principle, we have to fill known mass of the sample into the optical cell to achieve the specified average sample density within the cell. In order to attain some different density values, a part of the sample confined in the optical cell has to be expanded into the expansion cell (B) at prescribed temperature in the single-phase region. The rocking device mentioned above is effective in maintaining the densities in three vessels unchanged before and after the sample expansion.

Temperature is measured by means of a 25Ω standard platinum resistance thermometer (M) calibrated against the ITS-90 and it is installed near the optical cell in the thermostated fluid bath (I). Special caution was paid to establish a uniform temperature field for a certain period of time in order to maintain well-established thermal equilibrium condition. In order to keep temperature constant, this standard platinum resistance thermometer detects the temperature fluctuation and then the

temperature of the thermostated bath fluid is maintained by the PID controller (S) within ±2 mK over several hours. Therefore we believe the sample temperature is equal to the bath fluid temperature when the thermal equilibrium has been well established.

We have evaluated the experimental uncertainties on the basis of the ISO recommendation[15] associated with a coverage factor of 2. The expanded uncertainty of the saturation density measurements varies from 0.5 to 4.0 $kg \cdot m^{-3}$, whereas that of the saturation temperature is ± 12 mK,

The purity of the sample used for the measurements is 99.9967 mol% for $CF_3CF_2OCH_3$. The sample has been analyzed by the RITE and no further purification has been applied in the present study.

**Results**

Concerning $CF_3CF_2OCH_3$, we have obtained 10 saturated-vapor density data and 13 saturated-liquid density data in the critical region. The experimental results are given in Table 1 where $\rho''$ denotes the saturated-vapor density and $\rho'$ the saturated-liquid density. The uncertainty of the temperature measurements depends upon the fluctuation of the thermostated bath temperature, the reliability of the thermometer, and the individual error with respect to the determination of the meniscus-disappearing temperature. The uncertainty of the temperature measurements is estimated to be within ±12 mK. The uncertainty of the density measurements depends upon the number of expansion procedures and varies from 0.5 to 4.0 $kg \cdot m^{-3}$, as shown in Table 1. Figure 2 summarizes the present results on a temperature-density diagram together with the saturation

densities measured by Tsuge *et al.*[16]

The critical opalescence was observed at 13 measurements for the densities between 449.9 and 590.6 $kg \cdot m^{-3}$. These measurements are given with an asterisk for the measured density values in Table 1. For 8 saturated-vapor densities below 472.4 $kg \cdot m^{-3}$ the meniscus descended with increasing temperature and disappeared at the bottom of the optical cell. To the contrary, for 9 saturated-liquid densities above 546.3 $kg \cdot m^{-3}$, the meniscus ascended with increasing temperature and it disappeared at the top of the optical cell. At other 6 density values near the critical density, the meniscus disappeared without reaching either the top or bottom of the optical cell.

At the density of 506.0 $kg \cdot m^{-3}$, the critical opalescence in the liquid phase was observed more intensely than in the vapor phase. At this density the meniscus descended slightly before it disappeared. As a whole, the most intense critical opalescence was observed at the density of 509.9 $kg \cdot m^{-3}$, where the critical opalescence in the vapor phase was a little more intense than in the liquid phase. At this density the meniscus ascended slightly before it disappeared. On the basis of these observations, we considered that the density of 509.9 $kg \cdot m^{-3}$ was the saturated-liquid density but the closest density to the critical point among the present results. Therefore, the critical density should be between these two density values, and we determined it to be $\rho_C$ = 509 ± 3 $kg \cdot m^{-3}$

The critical temperature can be determined as the saturation temperature that corresponds to the critical density. As shown in Table 1, the temperature range corresponding to the density range between 506.0 and 510.1 $kg \cdot m^{-3}$ is in good agreement with each other within the uncertainty of the temperature measurements. Therefore, we determined the critical temperature to be $T_C$ = 406.830 ± 0.017 K.

## Discussion

For the critical density and temperature, the comparison between the present results and the literature values reported by Sako *et al.*[17] is presented in Table 2. The present critical temperature value agrees with the value reported by Sako *et al.*[17] within the mutual estimated uncertainties. The critical density reported by Sako *et al.*[17] is lower than our measurement by 10 kg·m$^{-3}$. The critical density value reported by Sako *et al.*[17] was exclusively obtained by their measurement at the critical point. On the other hand, we have performed our measurements over and over in the vicinity of the critical point, and the critical density was determined by a careful examination of the measured saturated-vapor and -liquid densities, which are extremely close to the critical point. Besides, the purity of the sample by Sako *et al.*[17] was 99.99 mol%, while we used the sample with the purity of 99.9967 mol%. Therefore, we believe our results would be far reliable.

The critical exponent, $\beta$, is used to represent the vapor-liquid coexistence curve in the critical region by means of the following power-law representation:

$$(\rho' - \rho'')/2\rho_C = B[(T_C - T)/T_C]^{\beta} \qquad (1)$$

where $\rho_C$ is the critical density, $T_C$ the critical temperature, single and double primes denote saturated-vapor and -liquid phase, respectively, and $B$ is the critical amplitude. Equation 1 requires isothermal pairs of liquid and vapor density values. Therefore, we

used the following correlation for the calculation of the corresponding saturated-vapor and -liquid densities,

$$\Delta\rho^* = \mathrm{D}_0\left|\Delta T^*\right|^{(1-\alpha)} + \mathrm{D}_1\left|\Delta T^*\right| + \mathrm{D}_2\left|\Delta T^*\right|^{(1-\alpha+\Delta_1)} \pm \mathrm{B}_0\left|\Delta T^*\right|^{\beta} \pm \mathrm{B}_1\left|\Delta T^*\right|^{(\beta+\Delta_1)} \quad (2)$$

where $\Delta\rho^* = (\rho - \rho_C)/\rho_C$ , $\left|\Delta T^*\right| = (T - T_C)/T_C$ , $\alpha$ and $\beta$ are the critical exponents, and $T$ is the temperature in Kelvin. The exponent $\Delta_1$ stands for the first symmetric correction-to-scaling exponent of the Wegner expansion (Levelt Sengers and Sengers[18]). From the theoretical background of eq 2, these exponents are $\alpha$ = 0.1085, $\beta$ = 0.325, and $\Delta_1$ = 0.50 (Levelt Sengers and Sengers[18]). The critical parameters in eq 2 are those determined in this study being $T_C$ = 406.830 K and $\rho_C$ = 509 kg·m$^{-3}$. On the basis of the present measurements and available saturation density data reported by Tsuge *et al.*[16], the coefficients $D_0$, $D_1$, $D_2$, $B_0$, and $B_1$ in eq 2 were determined by the least-squares fitting as summarized in Table 3. In this least-squares fitting, we have used 28 data including 16 present data and 12 data points by Tsuge *et al.*[16] as a set of input data, by excluding 7 present measurements in the very vicinity of the critical point corresponding to $|\Delta T^*| < 6.0 \bullet 10^{-5}$. The upper sign "+" and the lower sign "–" of the fourth and fifth term in eq 2 correspond to the saturated-liquid and - vapor, respectively. Equation 2 is effective for the range of densities between 75.0 and 854.2 kg·m$^{-3}$. The vapor-liquid coexistence curve calculated from eq 2 is shown in Figure 2. The density deviations of the present measurements and the measurements reported by Tsuge *et al.*[16] from eq 2 are illustrated in Figure 3. Equation 2 reproduces the input data among the present measurements and the measurements reported by Tsuge *et al.*[16] within ± 2.3 %

in density.

Figure 4 shows a logarithmic plot between $(\rho - \rho_C)/2\rho_C$ and $|\Delta T^*|$ in terms of the present measurements and calculated results from eq 2. The power-law representation, eq 1, suggests that a straight line can fit the experimental results satisfactorily. The slope of the straight line is equivalent to the critical exponent, $\beta$. For the determination of the critical exponent, $\beta$, and the critical amplitude, $B$, we used the data utilized for determination of the coefficients in eq 2. As a result of the least-squares fitting, the values of $\beta$ and $B$ were obtained being $\beta$ = 0.324 and $B$ = 1.89. The $\beta$ value is close to the theoretical value of 0.325 (Levelt Sengers and Sengers[18]).

## Conclusions

By means of visual observation of the meniscus in the optical cell, 10 saturated vapor and 13 liquid densities of pentafluoroethyl methyl ether in the critical region were measured, and the critical density, critical temperature, critical exponent, and the critical amplitude were determined. Saturated vapor-liquid density correlation for this fluorinated ether was also developed on the basis of the present measurements.

## Acknowledgment

The present study was partially supported by the New Energy and Industrial Technology Development Organization (NEDO), Tokyo, Japan through the RITE. We

are grateful to the RITE for furnishing the research-grade samples.

**Literature Cited**


(1) Sekiya, A.; Misaki, S.; A Continuing Search for New Refrigerants. *Chmtech* **1996**, *26*, 44-48.

(2) Okazaki, S.; Higashi, Y.; Takaishi, Y.; Uematsu, U.; Watanabe, K. Procedures for Determining the Critical Parameters of Fluids. *Rev. Sci. Intrum.* **1983**, *54*, 21-25.

(3) Tanikawa, S.; Kabata, Y.; Sato, H.; Watanabe, K. Measurements of the Critical Parameters and the Vapor-Liquid Coexistence Curve in the Critical Region of HCFC-123. *J. Chem. Eng. Data* **1990**, *35*, 381-385.

(4) Higashi, Y.; Uematsu, M.; Watanabe, K. Determination of the Vapor-Liquid Coexistence Curve and the Critical Parameters for Refrigerant 502. *Int. J. Thermophys.* **1984**, *5*, 117-130.

(5) Higashi, Y.;Okazaki, S.; Takaishi, Y.; Uematsu, M.; Watanabe, K. Measurements of the Vapor-Liquid Coexistence Curve for the Binary R 12 + R 22 System in the Critical Region. *J. Chem. Eng. Data* **1984**, *29*, 31-36.

(6) Higashi, Y.; Uematsu, M.; Watanabe, K. Measurements of the Vapor-Liquid Coexistence Curve and the Critical Locus for Several Refrigerant Mixtures. *Int. J. Thermophys.* **1986**, *7*, 29-40.

(7) Higashi, Y.; Ashizawa, M.; Kabata, Y.; Majima T.; Uematsu, M.; Watanabe, K. Measurements of Vapor Pressure, Vapor-Liquid Coexistence Curve and Critical Parameters of Refrigerant 152a. *JSME Int. J.* **1987**, *10*, 1106-1112.

(8) Higashi, Y.; Kabata, Y.; Uematsu, M.; Watanabe, K. Measurements of the Vapor-Liquid Coexistence Curve for the R13B1 + R114 System in the Critical Region. *J. Chem. Eng. Data* **1988**, *33*, 23-26.

(9) Kabata, Y.; Tanikawa, S.; Uematsu, M.; Watanabe, K. Measurements of the Vapor-Liquid Coexistence Curve and the Critical Parameters for 1,1,1,2-Tetrafluoroethane. *Int. J. Thermophys.* **1989**, *10*, 605-616.

(10) Tanikawa, S.; Tatoh, J.; Maezawa Y.; sato, H.; Watanabe, K. Vapor-Liquid Coexistence Curve and the Critical Parameters of 1-Chloro-1,1-Difluoroethane (HCFC-142b). *J. Chem. Eng. Data* **1992**, *37*, 74-76.

(11) Tatoh, J.; Kuwabara, S.; Sato, H.; Watanabe, K. Measurements of the Vapor-Liquid Coexistence Curve in the Critical Region and the Critical Parameters of 1,1,2,2-Tetrafluoroethane. *J. Chem. Eng. Data* **1993**, *38* 116-118.

(12) Kuwabara, S.; Aoyama, H.; Sato, H.; Watanabe, K. Vapor-Liquid Coexistence Curves in the Critical Region and the Critical Temperatures and Densities of Difluoromethane and Pentafluoroethane. *J. Chem. Eng. Data* **1995**, *40*, 112-116.

(13) Aoyama, H.; Kishizawa, G.; Sato, H.; Watanabe, K. Vapor-Liquid Coexistence Curves in the Critical Region and the Critical Temperatures and Densities of 1,1,1,2-Tetrafluoroethane (R-134a), 1,1,1-Trifluoroethane (143a), and 1,1,1,2,3,3-Hexafluoropropane (R-236ea). *J. Chem. Eng. Data* **1996**, *41*, 1046-1051.

(14) Kishizawa, G.; sato, H.; Watanabe, K. Measurements of Saturation Densities in Critical Region and Critical Loci Binary R32/125 and R-125/143a Systems. *International Journal of Thermophysics* **1999**, *20*, 923-932.

(15) International Organization for Standardization. *Guide to the Expression of Uncertainty in Measurement*, ISO: Switzerland, **1993**.

(16) Tsuge, T.; Sato, H.; Watanabe K. Vapor Pressure and *PVT* Properties of HFE-245mc (pentafluoroethyl methyl ether). *Rev. High Pressure Sci. Technol*. **1998**, *7*, 1198-1200.

(17) Sako, T.; Sato, M.; Nakazawa, N.; Oowa, M.; Yasumoto, M.; Ito, H.; Yamashita, S. Critical Properties of Fluorinated Ethers. *J. Chem. Eng. Data* **1996**, *41*, 802-805.

(18) Levelt Sengers, J. M. H.; Sengers, J. V. In *Perspectives in Statistical Physics*, Raveche, H. J., Ed.; North-Holland: Amsterdam, **1981**; Chapter 14.

**Table 1. Saturated-Vapor and -Liquid Densities of 245cbEβγ**

| $\rho''$/ kg·m$^{-3}$ | $T$ / K | $\rho'$ / kg·m$^{-3}$ | $T$ / K |
|---|---|---|---|
| 324.9 ± 0.7 | 404.708 | 509.9 ± 0.5* | 406.834 |
| 348.8± 2.2 | 405.629 | 510.1 ± 3.2* | 406.829 |
| 365.8 ± 2.7 | 405.984 | 515.5 ± 1.9* | 406.814 |
| 373.5 ± 1.4 | 406.125 | 542.0 ± 0.6* | 406.819 |
| 400.1 ± 0.5 | 406.465 | 546.3 ± 2.0* | 406.799 |
| 441.1 ± 4.0 | 406.769 | 552.2 ± 0.6* | 406.774 |
| 449.4 ± 4.0* | 406.809 | 573.1 ± 3.6* | 406.723 |
| 472.4 ± 3.0* | 406.804 | 585.2 ± 0.6* | 406.612 |
| 481.3 ± 3.0* | 406.809 | 590.6 ± 3.7* | 406.592 |
| 506.0 ± 1.9* | 406.824 | 604.9 ± 0.6 | 406.500 |
| | | 613.9 ± 2.2 | 406.323 |
| | | 632.6 ± 2.3 | 405.994 |
| | | 657.5 ± 0.6 | 405.487 |

* Density values with an asterisk were obtained when the critical opalescence was observed.

**Table 2. Comparison of the Critical Temperature and Density**

| author | $T_C$ / K | $\rho_C$ / kg·m$^{-3}$ | Sample purity |
|---|---|---|---|
| Sako *et al.*[17] | 406.80 ± 0.03 | 499 ± 1 | 99.9 mol% |
| This work | 406.830 ± 0.017 | 509 ± 3 | 99.9967 mol% |

**Table 3. Numerical Constants in eq 2**

| $D_0$ | $D_1$ | $D_2$ | $B_0$ | $B_1$ |
|---|---|---|---|---|
| -7.65338 | 13.3526 | -7.41279 | 1.95950 | -0.384531 |

**Figure Captions**

**Figure 1.** Experimental apparatus: A, optical cell; B, expansion vessel; C, supplying vessel; H1, main heater; H2, sub heater; I, thermostated bath; L, stirrer; M, platinum resistance thermometer; N, thermometer bridge; S, PID controller; T, voltage converter; V, valves.

**Figure 2.** Vapor-liquid coexistence curve of $CF_3CF_2OCH_3$: ●, this work; Δ, Tsuge *et al.*[16]; *, critical point.

**Figure 3.** Density deviation from eq 2: ○, this work (saturated vapor density); ●, this work (saturated liquid density); Δ, Tsuge *et al.*[16] (saturated vapor density); ▲, Tsuge *et al.*[16] (saturated liquid density).

**Figure 4.** Critical exponent and amplitude: ○, this work (saturated vapor density); ●, this work (saturated liquid density); Δ, Tsuge *et al.*[16] (saturated vapor density); ▲, Tsuge *et al.*[16] (saturated liquid density); $\beta = 0.324$; $B = 1.89$.

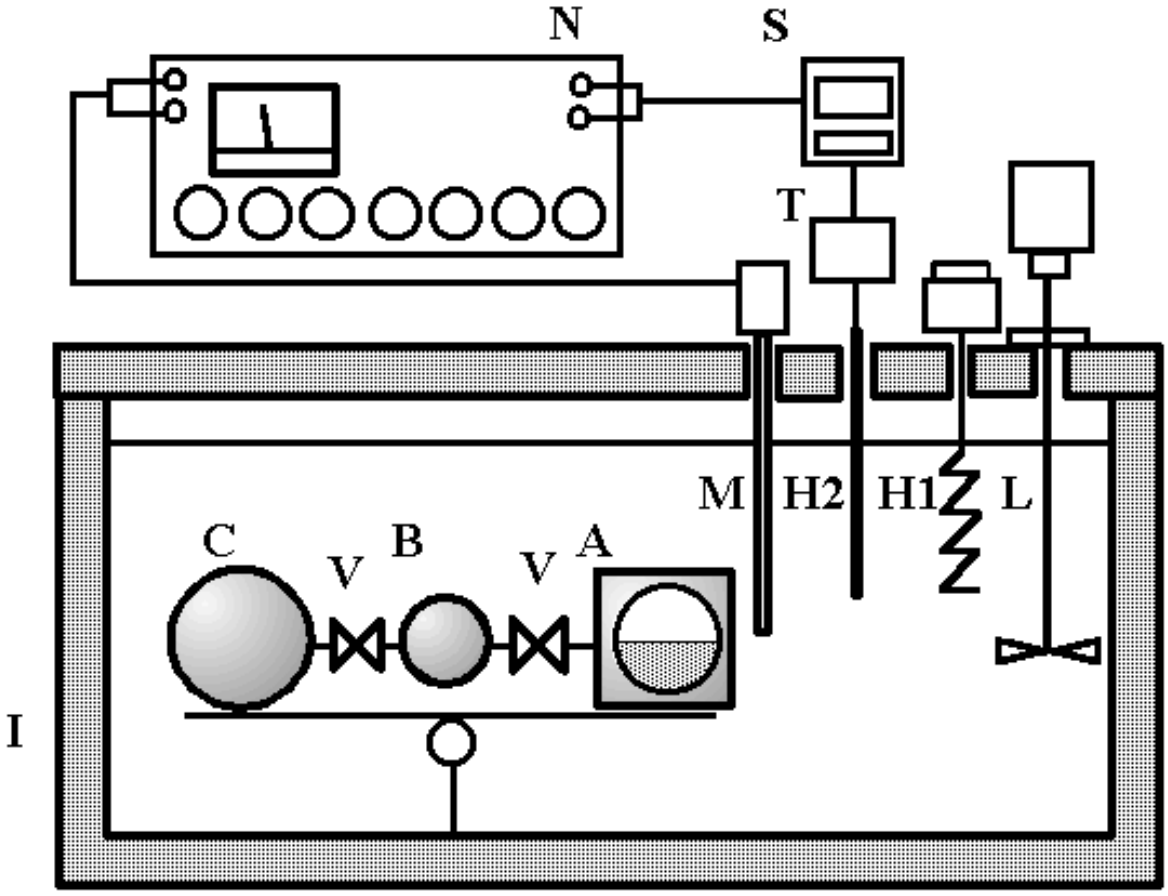


**Figure 1.** Experimental apparatus: A, optical cell; B, expansion vessel; C, supplying vessel; H1, main heater; H2, sub heater; I, thermostated bath; L, stirrer; M, platinum resistance thermometer; N, thermometer bridge; S, PID controller; T, voltage converter; V, valves.

Yoshii *et al.*

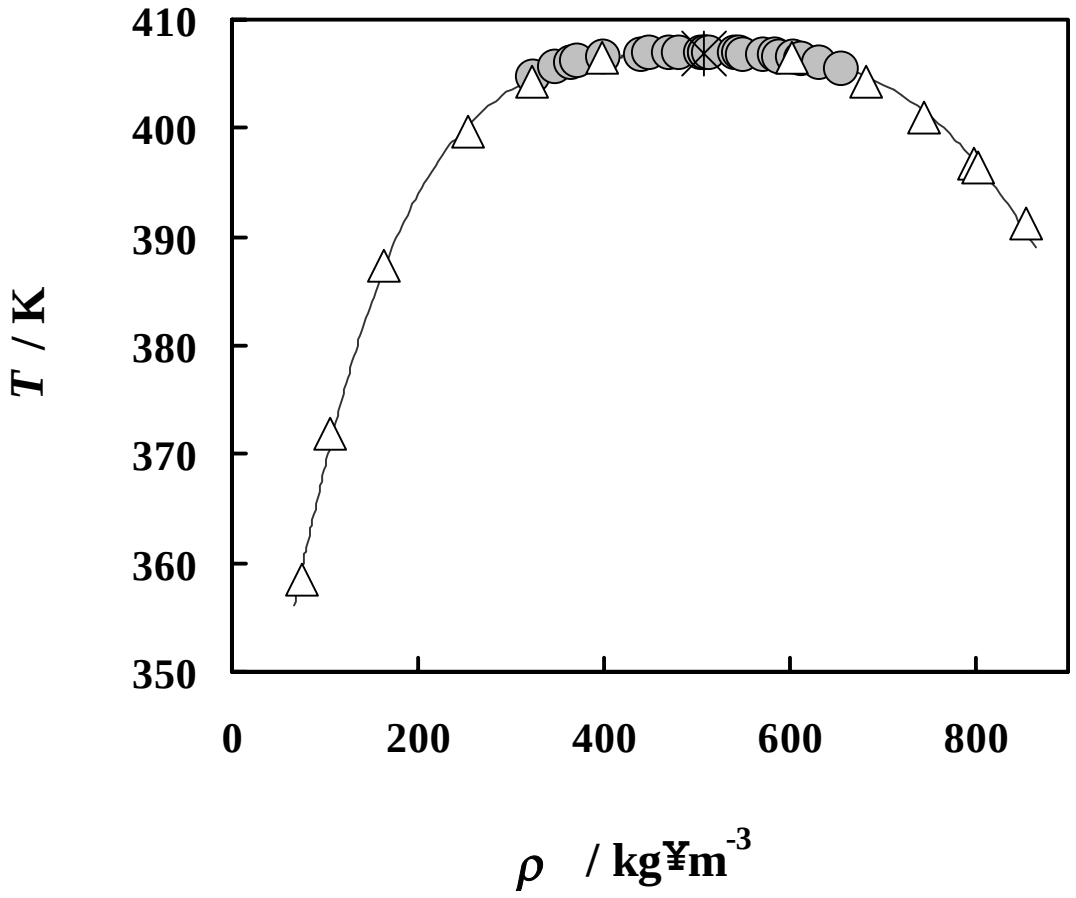


**Figure 2.**. Vapor-liquid coexistence curve of $CF_3CF_2OCH_3$: ●, this work; Δ, Tsuge *et al.*[16]; *, critical point.

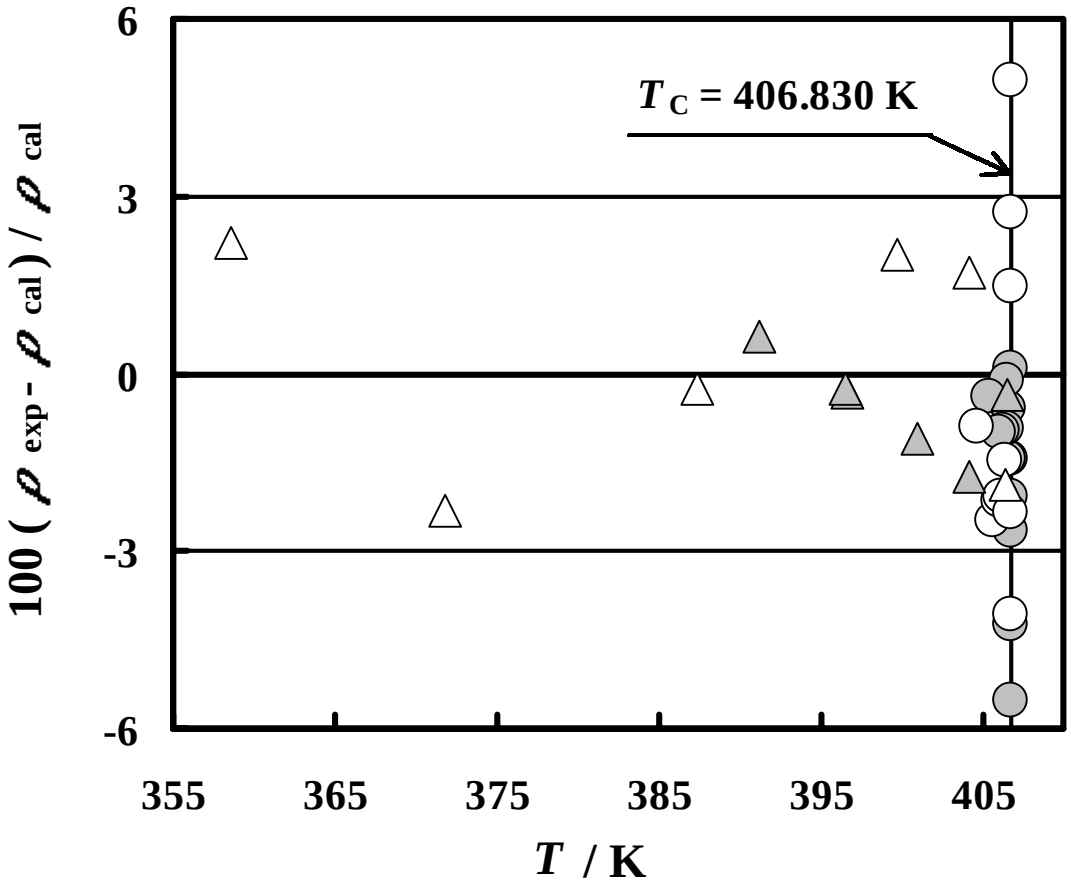


**Figure 3.** Density deviation from eq 2: ○, this work (saturated vapor density); ●, this work (saturated liquid density); Δ, Tsuge *et al.*[16] (saturated vapor density); ▲, Tsuge *et al.*[16] (saturated liquid density).

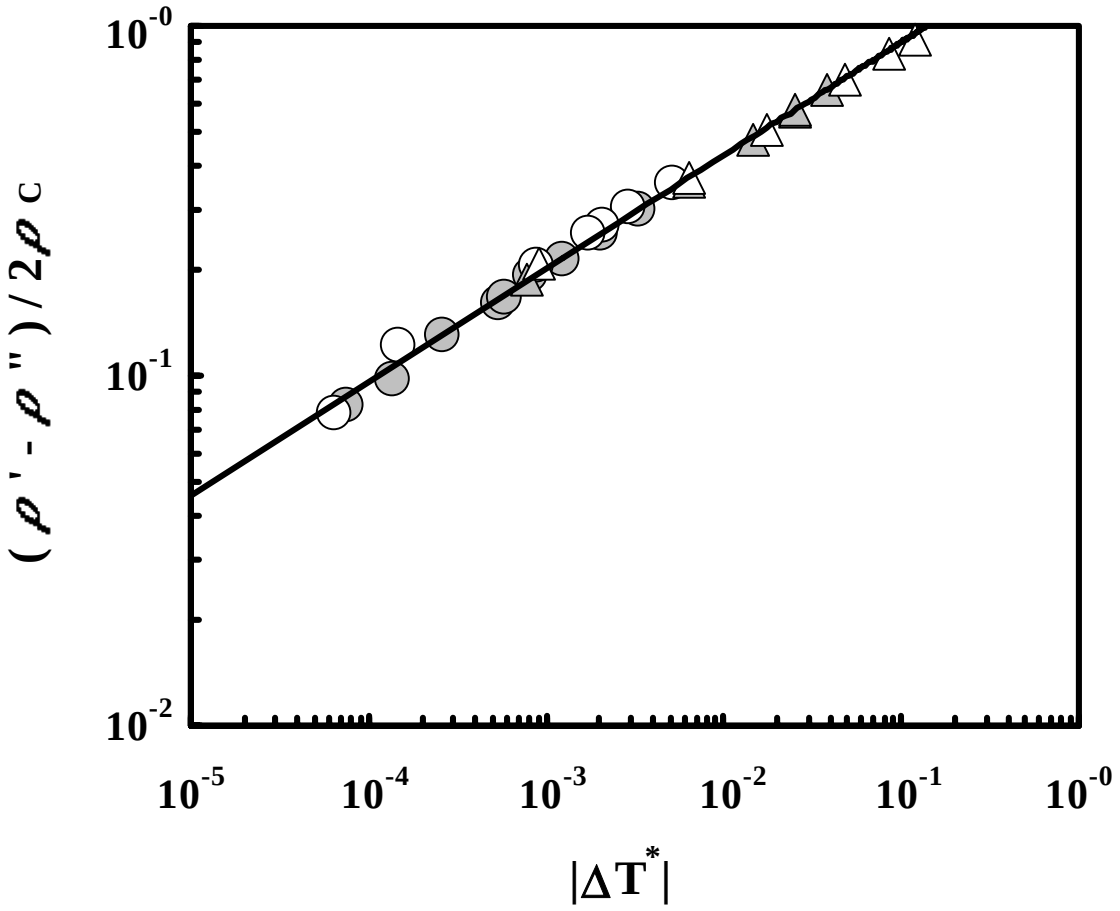


**Figure 4.** Critical exponent and amplitude: ○, this work (saturated vapor density); ●, this work (saturated liquid density); Δ, Tsuge *et al.*[16] (saturated vapor density); ▲, Tsuge *et al.*[16] (saturated liquid density); $\beta = 0.324$; $B = 1.89$.